Doping of Ga_2O_3 with transition metals

H. Peelaers* and C. G. Van de Walle
Materials Department, University of California, Santa Barbara, California 93106-5050, USA
(Received 4 August 2016; revised manuscript received 20 October 2016; published 10 November 2016)

We explore the viability of using transition-metal impurities as *n*-type dopants in β-Ga_2O_3, focusing on W, Mo, Re, and Nb. Our first-principles calculations show that these impurities can incorporate on both crystallographically inequivalent Ga sites, with the octahedrally coordinated sites being preferred. Mo and Re behave as deep donors. Tungsten on a tetrahedral site is a shallow donor, but unfortunately W on an octahedral site is much lower in energy. Niobium emerges as the best candidate for *n*-type doping: It has a low formation energy, is a shallow donor on the tetrahedral site, and has only a modest ionization energy (0.15 eV) on the octahedral site.

DOI: 10.1103/PhysRevB.94.195203

I. INTRODUCTION

Ga_2O_3 is a transparent conducting oxide with a wide variety of applications. Given its particularly wide band gap (∼4.8 eV [1,2]), it can be used as a contact for solar cells [3,4], light emitters, or detectors [5] with transparency well into the ultraviolet. It is also a promising material for high-power electronics: high-voltage metal-semiconductor field-effect transistors [6], nanomembrane field-effect transistors [7], and Schottky barrier diodes [8] have already been demonstrated. Ga_2O_3 can also be used as a gas sensor [9]. Ga_2O_3 crystals occur in multiple polymorphs, of which the monoclinic β polymorph is the most stable for a large range of temperatures. The conventional unit cell of β-Ga_2O_3 is shown in Fig. 1. It contains two inequivalent Ga positions: a tetrahedrally coordinated Ga(I) and an octahedrally coordinated Ga(II) position. There are also three inequivalent O positions, as labeled in Fig. 1.

The as-grown material is usually unintentionally *n*-type. This cannot be attributed to oxygen vacancies, which are deep donors with a very large ionization energy [10]. Calculations for various dopant impurities have already been performed [10,11]; Si, Ge, Sn, or C on Ga sites or Cl and F on O sites have been found to be shallow donors. However, experimental results have shown smaller than expected conductivity upon doping with Si or Sn [12–15].

In this work we consider doping with transition metals. Recent experiments [16,17] have shown that it is possible to incorporate a large concentration of W in β-Ga_2O_3 (up to 30.4% W to Ga ratio), without the formation of WO_3 phases, and without phase transitions to one of the other Ga_2O_3 phases. Here we perform a detailed study of the effect of W doping in Ga_2O_3 using density functional theory (DFT) with a hybrid functional. In order to present a fuller picture of the effects of doping with transition metals, we also examine Mo, Nb, and Re.

II. METHODOLOGY

Our calculations are based on DFT using PAW pseudopotentials [18] in a plane-wave basis set with an energy cutoff of 400 eV, using the Vienna *Ab initio* Simulation Package (VASP) code [19]. A $1 \times 3 \times 2$ supercell based on the (20-atom) conventional unit cell of Ga_2O_3 is used to simulate an isolated defect. This 120-atom supercell is sampled using a $2 \times 2 \times 2$ *k*-point grid. We use the HSE06 hybrid functional [20,21], with a mixing parameter of 35% to accurately produce the electronic band structure of Ga_2O_3 [22–24]. We find a direct band gap of 4.88 eV and an indirect band gap of 4.84 eV, in good agreement with the experimental band gap of 4.76 eV [1,2]. This functional also provides a very good description of the structural properties of β-Ga_2O_3, as can be seen from the comparison made with experimental lattice parameters [25,26] in Table I.

The formation energy of a defect or impurity is a key descriptor that determines its concentration, the stability of different charge states, and the electronic transition levels. For W on a Ga site (W_{Ga}) it is given by [27]

$$\begin{aligned} E^f\left(\mathrm{W}_{\mathrm{Ga}}^q\right) = {} & E_{\mathrm{tot}}\left(\mathrm{W}_{\mathrm{Ga}}^q\right) - E_{\mathrm{tot}}(\mathrm{Ga_2O_3}) \\ & - \left(\mu_{\mathrm{W}} + \mu_{\mathrm{W}}^0\right) + \left(\mu_{\mathrm{Ga}} + \mu_{\mathrm{Ga}}^0\right) \\ & + q(E_F + E_{\mathrm{VBM}}) + \Delta^q, \end{aligned} \tag{1}$$

where $E_{\mathrm{tot}}(W_{\mathrm{Ga}}^q)$ is the total energy of one W_{Ga} in charge state q in the supercell, $E_{\mathrm{tot}}(Ga_2O_3)$ is the energy of the undoped supercell, and E_F is the Fermi energy, referenced with respect to the valence-band maximum (VBM) E_{VBM}. The term Δ^q corrects for the spurious interaction of charged defects caused by using periodic boundary conditions [28,29]. The chemical potentials μ_{W} and μ_{Ga} are referenced to the total energy per atom of the bulk metals [$\mu_{\mathrm{W}}^0 = E_{\mathrm{tot}}(\mathrm{W})$, $\mu_{\mathrm{Ga}}^0 = E_{\mathrm{tot}}(\mathrm{Ga})$], and μ_{O} is referenced to the energy of an O atom in an O_2 molecule [$\mu_{\mathrm{O}}^0 = 1/2 E_{\mathrm{tot}}(\mathrm{O_2})$]. The Ga and O potentials have to fulfill the stability condition for bulk Ga_2O_3:

$$2\mu_{\mathrm{Ga}} + 3\mu_{\mathrm{O}} = \Delta H_f(\mathrm{Ga_2O_3}), \tag{2}$$

where $\Delta H_f(Ga_2O_3)$ is the formation enthalpy of bulk Ga_2O_3 (−10.73 eV), as well as $\mu_{\mathrm{W}} \leqslant 0$ and $\mu_{\mathrm{Ga}} \leqslant 0$. We will present our results for two limiting cases: Ga-rich ($\mu_{\mathrm{Ga}} = 0$) and Ga-poor ($\mu_{\mathrm{O}} = 0$) conditions. The W chemical potential will determine the doping level, but the solubility limit is set by

$$\mu_{\mathrm{W}} + 3\mu_{\mathrm{O}} = \Delta H_f(\mathrm{WO_3}), \tag{3}$$

where $\Delta H_f(WO_3)$ is the calculated formation enthalpy of WO_3 (−7.93 eV). For the other transition metals, the solubility limits are set by the calculated enthalpies of MoO_3

*peelaers@engineering.ucsb.edu

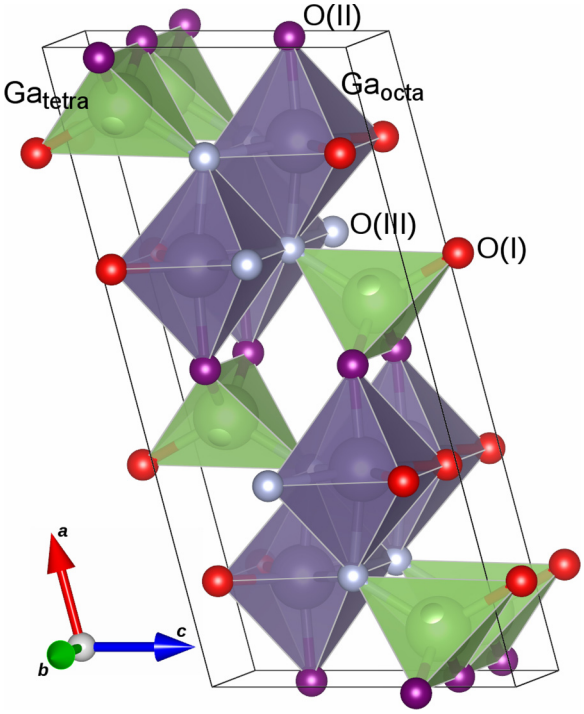

FIG. 1. The conventional unit cell of monoclinic β-Ga_2O_3. The two inequivalent Ga sites (large spheres) and the three inequivalent O sites (smaller spheres) are indicated. The Ga sites are labeled as tetrahedral (Ga_{tetra}), corresponding to a Ga(I) site, and octahedral (Ga_{octa}), corresponding to a Ga(II) site.

(−6.69 eV), Re_2O_7 (−12.81 eV), NbO_2 (−7.92 eV), and Nb_2O_5 (−18.82 eV). The charge-state transition level (q/q') can be estimated from the formation energies by

$$(q/q') = \frac{E^f\left(W_{Ga}^q; E_F = 0\right) - E^f\left(W_{Ga}^{q'}; E_F = 0\right)}{(q' - q)}. \quad (4)$$

When the Fermi level is below this energy, the charge state q is stable; otherwise, the charge state q' is stable.

III. RESULTS AND DISCUSSION

We first consider W incorporation on Ga sites in Ga_2O_3. The different bonding environments of the two inequivalent Ga sites, with the Ga(I) site tetrahedrally coordinated and the Ga(II) site octahedrally coordinated can lead to different formation energies and charge-state transition levels. An isolated W atom has four 5*d* and two 6*s* electrons. These electrons are all valence electrons and thus available for bonding, explaining the +6 oxidation state state of W in WO_3. Gallium, on the other hand, has two 4*s* and one 4*p* electrons, and a +3 oxidation state. Substituting W on a Ga site thus provides three additional electrons, turning W into a potential triple donor. This is confirmed by the calculated formation energies, shown in Fig. 2. The formation energy of W_{Ga} is lower under Ga-rich conditions than under O-rich conditions. This may seem surprising for an impurity that substitutes on the Ga site, but it is caused by our choice to depict the formation energies for conditions corresponding to the solubility limit, which is set by Eq. (3) and introduces a dependence of μ_W on μ_O.

Tungsten on the tetrahedral site acts as a shallow donor: for Fermi levels high in the gap it occurs in a 1+ charge state, indicating that it always donates an electron to the conduction band. We find that the (1+/0) transition level occurs at 0.15 eV above the conduction-band minimum (CBM). For Fermi levels lower in the gap, the 2+ and 3+ charge states are stable. $W_{Ga,tetra}$ can thus, in principle, lead to *n*-type doping of Ga_2O_3. Tungsten on the octahedral site, on the other hand, acts as a deep donor: It assumes a neutral charge state for Fermi levels within 0.54 eV of the CBM.

Unfortunately, the formation energy of W on the octahedral site is significantly lower than that on the tetrahedral site; at the CBM (*n*-type conditions) the energy difference between the two sites is 1.82 eV. This difference is related to the fact that the charge-state transition levels occur at lower Fermi-level positions in the case of the octahedral site. For the octahedral site the (3+/2+), (2+/1+), and (1+/0) transition levels occur at 1.87 eV, 3.06 eV, and 4.30 eV above the VBM, respectively; for the tetrahedral site (3+/2+) occurs at 2.34 eV and (2+/1+) at 3.44 eV. Different transition levels are to be expected, since the different bonding environment (octahedral

TABLE I. Calculated and experimental lattice parameters and band gap of β-Ga_2O_3.

	Calculated	Experimental
a (Å)	12.27	12.21[a]
b (Å)	3.05	3.04[a]
c (Å)	5.82	5.80[a]
β	103.82°	103.83°[a]
E_{gap}^{direct} (eV)	4.88	4.76[b]
$E_{gap}^{indirect}$ (eV)	4.84	

[a]Refs. [25,26].
[b]Refs. [1,2].

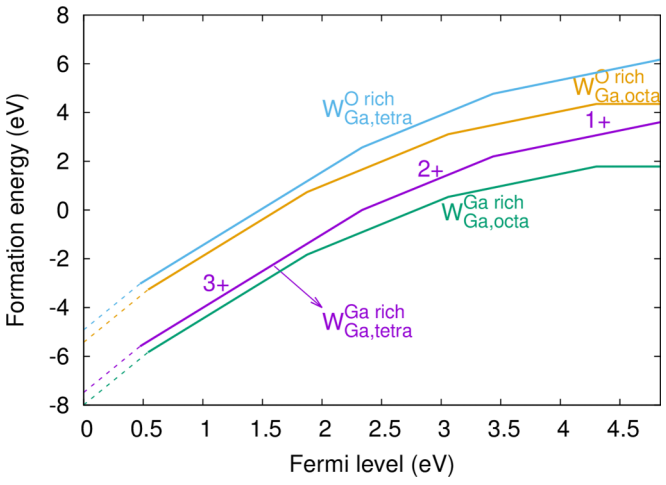

FIG. 2. Formation energy diagram of substitutional W (W_{Ga}) on the two inequivalent Ga sites in Ga_2O_3. The superscript indicates if Ga rich or O rich conditions are assumed. The zero of Fermi energy is at the VBM. The labels 3+, 2+, and 1+ shown on the curves for Ga-rich conditions and the tetrahedral site, indicate the charge state; the slope reflects the charge state. The dashed lines, with a slope of 4+, indicate the presence of a 3+ charge state with a hole polaron.

versus tetrahedral), leads to a different crystal field, which leads to a different character of the d orbitals in the band gap. The local distortion around the W atom also contributes to the energy difference. In bulk Ga_2O_3, the bond lengths of the octahedral site are longer than the bond lengths of the tetrahedral site. The 0 and 1+ charge state of W leads to a local distortion where the bond lengths are increased: on average by 5.0% (1.8%) for the octahedral site and 6.4% (3.6%) for the tetrahedral site for the 0 (1+) charge state. This larger distortion for the tetrahedral site compared to the octahedral site can explain why the formation energies for the same charge states are higher in the case of the tetrahedral site. For larger charge states (2+ and 3+), the difference between both sites decreases to an average of 0.3%, explaining why the formation energy difference between both sites is smaller for these charge states.

Depending on the charge state, various numbers of electrons occupy the d states of W, giving rise to a magnetic moment. For the 3+ charge state it is 0 μ_B, and it increases with decreasing charge state. For the 0 charge state the magnetic moment is 3 μ_B. These magnetic moments are observed for both the octahedral and the tetrahedral sites. This also implies that the W high-spin state is always preferred. The total magnetic moment is mostly located on the W atom, with electrons residing in the W 5d states. This is confirmed by inspection of the spin density (the difference in density corresponding to spin-up and spin-down states) in Fig. 3; the figure does not include the spin density of the 3+ charge state, since it is zero (magnetic moment 0 μ_B). An analysis of the orbital-projected character of the bands shows that W d states are mixed with a small contribution from O p states.

The "4+" charge state, whose formation energies are shown using dashed lines in Fig. 2 and whose spin density is shown in Fig. 3(a), does not correspond to a true 4+ charge state. It is actually a 3+ charge state, together with a hole polaron localized on O(II) atoms, as evident from the spin density. The

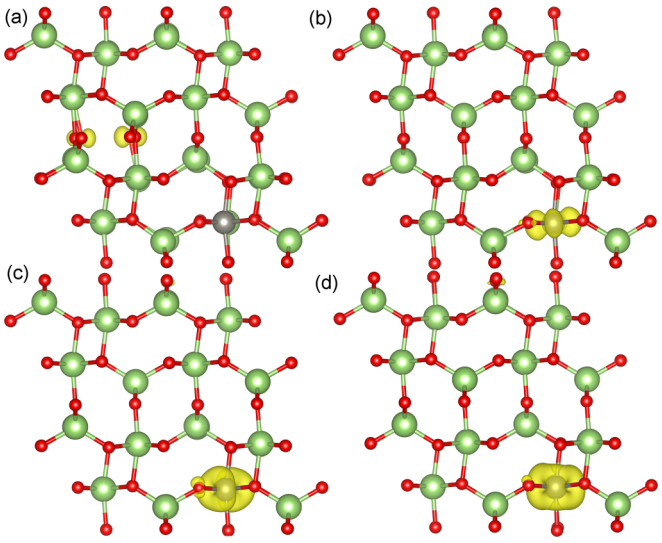

FIG. 3. Spin density for a W donor on an octahedrally coordinated Ga(II) site for (a) the 4+ (1 μ_B), (b) the 2+ (1 μ_B), (c) the 1+ (2 μ_B), and (d) the 0 charge state (3 μ_B). Isosurfaces are drawn at 10% of the maximum density.

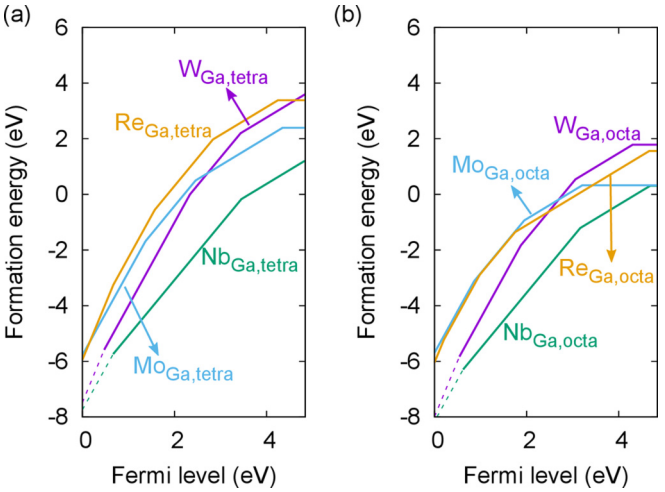

FIG. 4. Formation energy diagram of substitutional W, Mo, Re, and Nb on Ga sites for Ga-rich conditions for (a) tetrahedral [Ga(I)] sites, and (b) octahedral [Ga(II)] sites. Dashed lines indicate the presence of hole polarons.

appearance of polarons is not surprising, as hole polarons are easily formed in bulk Ga_2O_3 [30].

We also considered other transition metals as dopants: Mo, which is isovalent with W, Nb, which has one fewer valence electron, and Re, which has one additional valence electron. The calculated formation energies in the case of Ga-rich conditions are shown in Fig. 4. Similar to W doping, the octahedral site is lower in energy compared to the tetrahedral site for all these dopants. For the isovalent Mo the (1+/0) transitions occur at 0.49 eV (tetrahedral) and 1.63 eV (octahedral) below the CBM; Mo is therefore a deep donor. For Re the levels occur at 0.59 eV (tetrahedral) and at 0.18 eV (octahedral) below the CBM. The latter is a low enough ionization energy for $Re_{Ga,octa}$ to be able to lead to n-type doping.

Niobium stands out: $Nb_{Ga,tetra}$ can be considered a shallow donor since the (1+/0) transition occurs only 0.03 eV below the CBM. For the octahedral site the (1+/0) transition occurs somewhat deeper in the gap, at 0.15 eV below the CBM, again low enough to enable n-type conductivity. Niobium also stands out because of its low formation energy (1.19 eV at the CBM for the tetrahedral site and 0.31 eV for the octahedral site, for Ga-rich conditions). Among the impurities considered here, Nb therefore emerges as the best candidate for transition-metal n-type doping of Ga_2O_3.

IV. CONCLUSIONS

In conclusion, we have studied doping of β-Ga_2O_3 with W, Mo, Nb, and Re. All these transition metals prefer high-spin states when incorporated on the Ga site. The unpaired electrons causing the magnetic moment have distinct d character. Substitution on the octahedral Ga sites is lower in energy compared to the Ga tetrahedral sites. These transition metals are generally deep donors. The main exception is Nb, which is a shallow donor when it substitutes on a tetrahedral site, and a small enough ionization energy to enable n-type conductivity on the octahedral site. Niobium also has the lowest formation energy among the considered transition metals.

ACKNOWLEDGMENTS

The authors acknowledge valuable feedback from M. L. Chabinyc. This work was supported by the MRSEC Program of the National Science Foundation (NSF) (DMR-1121053) and by the Army Research Office (W911NF-13-1-0380). Computing resources were provided by the Extreme Science and Engineering Discovery Environment (XSEDE), which is supported by National Science Foundation Grant No. ACI-1053575 (NSF DMR-070072N).

[1] H. H. Tippins, Phys. Rev. **140**, A316 (1965).
[2] T. Matsumoto, M. Aoki, A. Kinoshita, and T. Aono, Jpn. J. Appl. Phys. **13**, 1578 (1974).
[3] A. K. Chandiran, N. Tetreault, R. Humphry-Baker, F. Kessler, E. Baranoff, C. Yi, M. K. Nazeeruddin, and M. Grätzel, Nano Lett. **12**, 3941 (2012).
[4] T. Minami, Y. Nishi, and T. Miyata, Appl. Phys. Express **6**, 044101 (2013).
[5] T. Oshima, T. Okuno, and S. Fujita, Jpn. J. Appl. Phys. **46**, 7217 (2007).
[6] M. Higashiwaki, K. Sasaki, A. Kuramata, T. Masui, and S. Yamakoshi, Appl. Phys. Lett. **100**, 013504 (2012).
[7] W. S. Hwang, A. Verma, H. Peelaers, V. Protasenko, S. Rouvimov, H. G. Xing, A. Seabaugh, W. Haensch, C. G. Van de Walle, Z. Galazka, M. Albrecht, R. Fornari, and D. Jena, Appl. Phys. Lett. **104**, 203111 (2014).
[8] K. Sasaki, M. Higashiwaki, A. Kuramata, T. Masui, and S. Yamakoshi, IEEE Electron Device Lett. **34**, 493 (2013).
[9] A. Trinchi, W. Wlodarski, and Y. Li, Sensors Actuat. B **100**, 94 (2004).
[10] J. B. Varley, J. R. Weber, A. Janotti, and C. G. Van de Walle, Appl. Phys. Lett. **97**, 142106 (2010).
[11] J. L. Lyons, D. Steiauf, A. Janotti, and C. G. Van de Walle, Phys. Rev. Appl. **2**, 064005 (2014).
[12] D. Gogova, G. Wagner, M. Baldini, M. Schmidbauer, K. Irmscher, R. Schewski, Z. Galazka, M. Albrecht, and R. Fornari, J. Cryst. Growth **401**, 665 (2014).
[13] K. Takakura, S. Funasaki, I. Tsunoda, H. Ohyama, D. Takeuchi, T. Nakashima, M. Shibuya, K. Murakami, E. Simoen, and C. Claeys, Phys. B Condens. Matter **407**, 2900 (2012).
[14] F. Zhang, K. Saito, T. Tanaka, M. Nishio, and Q. Guo, J. Mater. Sci. Mater. Electron. **26**, 9624 (2015).
[15] D. Gogova, M. Schmidbauer, and A. Kwasniewski, Cryst. Eng. Comm. **17**, 6744 (2015).
[16] A. A. Dakhel, J. Mater. Sci. **47**, 3034 (2012).
[17] E. J. Rubio and C. V. Ramana, Appl. Phys. Lett. **102**, 191913 (2013).
[18] P. E. Blöchl, Phys. Rev. B **50**, 17953 (1994).
[19] G. Kresse and J. Furthmüller, Phys. Rev. B **54**, 11169 (1996).
[20] J. Heyd, G. E. Scuseria, and M. Ernzerhof, J. Chem. Phys. **118**, 8207 (2003).
[21] J. Heyd, G. E. Scuseria, and M. Ernzerhof, J. Chem. Phys. **124**, 219906 (2006).
[22] M. Mohamed, C. Janowitz, I. Unger, R. Manzke, Z. Galazka, R. Uecker, R. Fornari, J. R. Weber, J. B. Varley, and C. G. Van de Walle, Appl. Phys. Lett. **97**, 211903 (2010).
[23] C. Janowitz, V. Scherer, M. Mohamed, A. Krapf, H. Dwelk, R. Manzke, Z. Galazka, R. Uecker, K. Irmscher, R. Fornari, M. Michling, D. Schmeißer, J. R. Weber, J. B. Varley, and C. G. Van de Walle, New J. Phys. **13**, 085014 (2011).
[24] H. Peelaers and C. G. Van de Walle, Phys. Status Solidi B **252**, 828 (2015).
[25] S. Geller, J. Chem. Phys. **33**, 676 (1960).
[26] J. Åhman, G. Svensson, and J. Albertsson, Acta Crystallogr. Sect. C **52**, 1336 (1996).
[27] C. Freysoldt, B. Grabowski, T. Hickel, J. Neugebauer, G. Kresse, A. Janotti, and C. G. Van de Walle, Rev. Mod. Phys. **86**, 253 (2014).
[28] C. Freysoldt, J. Neugebauer, and C. G. Van de Walle, Phys. Rev. Lett. **102**, 016402 (2009).
[29] C. Freysoldt, J. Neugebauer, and C. G. Van de Walle, Phys. Status Solidi B **248**, 1067 (2011).
[30] J. B. Varley, A. Janotti, C. Franchini, and C. G. Van de Walle, Phys. Rev. B **85**, 081109 (2012).